HHS Public Access

Evolution of Welding-Fume Aerosols with Time and Distance from the Source:

A study was conducted on the spatiotemporal variability in welding-fume concentrations for the characterization of first- and second-hand exposure to welding fumes

L. G. CENA,
West Chester University of Pa. and the Health Effects Laboratory Div. of the

B. T. CHEN, and
Health Effects Laboratory Div. of the National Institute for Occupational Safety and Health, and National Institute for Occupational Safety and Health, Morgantown, W.Va

M. J. KEANE
Health Effects Laboratory Div. of the National Institute for Occupational Safety and Health, and National Institute for Occupational Safety and Health, Morgantown, W.Va

L. G. CENA: LCena@wcupa.edu

Abstract

Gas metal arc welding fumes were generated from mild-steel plates and measured near the arc (30 cm), representing first-hand exposure of the welder, and farther away from the source (200 cm), representing second-hand exposure of adjacent workers. Measurements were taken during 1-min welding runs and at subsequent 5-min intervals after the welding process was stopped. Number size distributions were measured in real time. Particle mass distributions were measured using a micro-orifice uniform deposition impactor, and total mass concentrations were measured with polytetrafluorothylene filters. Membrane filters were used for collecting morphology samples for electron microscopy. Average mass concentrations measured near the arc were 45 mg/m^3 and 9 mg/m^3 at the farther distance. The discrepancy in concentrations at the two distances was attributed to the presence of spatter particles, which were observed only in the morphology samples near the source. As fumes aged over time, mass concentrations at the farther distance decreased by 31% (6.2 mg/m^3) after 5 min and an additional 13% (5.4 mg/m^3) after 10 min. Particle number and mass distributions during active welding were similar at both distances, indicating similar exposure patterns for welders and adjacent workers. Exceptions were recorded for particles smaller than 50 nm and larger than 3 μm, where concentrations were higher near the arc, indicating higher exposures of welders. These results were confirmed by microscopy analysis. As residence time increased, number concentrations decreased dramatically. In terms of particle number concentrations, second-hand exposures to welding fumes during active welding may be as high as first-hand exposures.

Keywords

Arc Welding; Exposure Assesment; Welding Aerosols; Spatiotemporal Variability; Morphology; Distance

Introduction

Several hazards have been associated with exposure to welding fume particles. These hazards are related to the high concentrations of aerosolized fine and ultrafine metal and metal oxide particles that are generated by the welding arc (Ref. 1). The heat generated by the arc melts the electrode, which is transferred to the welding pool in the form of superheated metal droplets. Spatter particles are also formed. The spatter particles and the heated metal droplets produce high concentrations of supersaturated metal vapors that then nucleate to form solid particles. As these particles cool to ambient temperatures, they undergo condensation and coagulation, which leads to the formation of chain aggregates and agglomerates (Ref. 2).

Welders work in numerous settings that range from outdoor, open, well-ventilated spaces (e.g., construction sites) to confined, poorly ventilated spaces (e.g., crawl spaces, ship hulls, and pipelines). The close proximity of the welder to the arc exposes the operator to high concentrations of metal fumes (Ref. 3); therefore, exposure studies usually measure fume concentrations in the welder's breathing zone (Refs. 4, 5). In recent years, researchers have placed increasing emphasis in studying the effects of exposure to specific fume constituents such as manganese, chromium, nickel, and other volatilized chemical species, and searching for ways to minimize exposure (Refs. 6–12).

A large amount of effort has also been placed in the development of exhaust ventilation systems to remove the welding fumes (Ref. 13). Some of these ventilation systems include extraction torches, local exhaust ventilation, and welding booths with built-in exhaust walls. In spite of these options, for practical or economic reasons, welding processes often occur in open spaces with no engineering controls, where nearby workers engaged in other tasks may also be exposed to the fumes (Ref. 3). This situation may be particularly prevalent in construction or manufacturing facilities where workers in multiple stations share the same large, open work area. Although, in general, efforts are made to shield the arc and to protect nearby workers from ultraviolet light exposure, often little is done to contain and prevent exposure from the fumes. This results not only in exposure of the welder to the welding fumes, but also in secondhand exposure of nearby workers. Second-hand exposure to welding fumes has not been investigated in the detail it deserves. This paper is a step in that investigation.

Prior studies have focused on the characterization of particle concentrations at relatively short distances from the arc. Zimmer and Biswas (Ref. 2) performed measurements between 5 and 20 cm from the welding arc in a stagnant chamber and reported spatial and temporal variations in particle number concentration within the chamber. They found that as distance from the arc increased, the average number concentration decreased up to fourfold between 5 and 20 cm. In our observations from field measurements (Ref. 3), we have estimated that

the breathing zone of the average welder is located at a distance of about 30 cm (12 in.) from the arc. Adjacent workers not directly involved in the welding process are expected to be at a distance of approximately 200 cm (6.5 ft) or more from the welder. We have designed a series of experiments to measure particle concentrations at these distances and compare exposures of welders with those of adjacent workers not directly involved in the welding process.

The objectives of this study were 1) to characterize the spatial and temporal variation in particle concentration and characteristics during gas metal arc welding (GMAW) simulated in a controlled environment, and 2) to estimate second-hand exposure of workers nearby a welding process in a restricted work environment.

Experimental Procedures

Experimental Setup

The experimental setup is shown in Fig. 1. Welding fumes were generated with a six-axis robotic arm welding machine (Lincoln Electric 100 iB, Cleveland, Ohio) capable of performing virtually continuous welding lines at constant speed, described in detail by Antonini et al. (Ref. 14). The welding machine was located inside a walk-in chamber measuring 2.5 m (width) by 3.5 m (depth) by 2.7 m (height). The robotic arm was equipped with a power supply (Lincoln Electric Power Wave 455), a water-cooled arc welding gun (450-A "Tough Gun," Tregaskiss, Windsor, ON, Canada) and an automatic wire feeder operated at 762 cm/min (300 in./min). Gas metal arc welding of A36 mild steel plates (0.64 cm thick) with mild steel wire (ER70S-3; Lincoln Electric, Cleveland, Ohio) was performed with the welding machine operated at 25.5 V and 220 A with 95% argon and 2% CO_2 shielding gas at 1.13 m^3/h (40 ft^3/h).

The experimental setup allowed for flexibility in changing sample locations and promoted steady-state generation of fumes in calm-air conditions. These conditions simulated welding in industrial facilities where no engineering controls, such as local exhaust ventilation, are used to capture the fumes, and in restricted work environments with minimal air movement.

The welding process generated an aerosol-laden plume. Air intake and outtake in the welding chamber were closed, and air movement and temperature in the chamber were measured with a hot-wire anemometer (Velocicalc 8346, TSI, Inc., Shoreview, Minn.). A movable sampling cart carried the instrumentation. Number size distribution for particles between 10 and 400 nm was measured with a scanning mobility particle sizer (SMPS, model 3080, TSI, Inc., Shoreview, Minn.) with 120-s measuring cycles and for particles between 500 nm and 10 μm with an aerodynamic particle sizer (APS, model 3321, TSI, Inc.). Due to the high concentration of the fumes, an aerosol diluter (Model 3302A, TSI, Inc.) was used to achieve a dilution ratio of 100 to 1 for the APS. A condensation particle counter (CPC, model 3007, TSI, Inc.) was used to monitor background particle concentrations. A micro-orifice uniform deposition impactor (MOUDI, Model 10, MSP Corp., Shoreview, Minn.) and a Nano-MOU-DI (Model 115, MSP Corp.) were combined and located inside the welding chamber to measure particle mass distribution. Particle collection with the combined MOUDI impactors ranged from 0.01 to ~32 μm separated in 15 fractions. Particle

mass concentrations were measured with 37-mm polytetrafluorothylene (PTFE) filters with 0.45-μm pore size (part # 225-17-04, SKC, Inc., Eight Four, Pa.) connected to a sampling pump (part # PCXR4, SKC, Inc.) operated at 4 L/min. Additional filter samples were collected for electron microscopy and particle morphology characterization on 47-mm Isopore polycarbonate membrane filters with 0.8-μm pore size (part # ATTP04700, EMD Millipore Corp., Billerica, Mass.) connected to a sampling pump (part # PCXR4, SKC, Inc.) operated at 1 L/min. The diameters of primary particles were measured using imaging software (ImageJ v1.48, National Institute of Health, Bethesda, Md.).

Sampling

Instruments' sampling probes and filters were located inside a 30-cm-long cylindrical plenum with 25 cm diameter and the open side located next to the welding arc at the same vertical location as the arc — Fig. 1. The plenum allowed for collection of fume samples for all aerosol measurement in the same relative location.

To evaluate the effect of temporal and spatial variation, particle size distribution and mass concentrations were measured at a fixed vertical position and two horizontal distances from the welding arc at different time intervals (T). First, concentrations were measured near the source at a distance of 30 cm (~12 in.). Concentrations at this distance represent firsthand exposures of a welding machine. Real-time instrument measurements were taken at T1 during a 1-min welding run after which the welding process was stopped and two additional measurements (T2 and T3) were taken at 150-s intervals. Collection of filter samples was started simultaneously at T1; morphology samples were collected for 15 s while mass concentration filter samples were collected for 5 min.

Concentrations were also measured farther away from the source, at a distance of 200 cm (~6.6 ft). Concentrations at this distance represent those of nearby workers not directly involved in the welding process. Measurements at this far distance were taken at T1 during a 1-min welding run after which the welding process was stopped and five additional measurements (T2–T6) were taken at 150-s intervals. The additional measurements after the welding process had stopped allowed for monitoring of particle size distribution as the fumes aged over time. One filter sample was collected at T1 for morphology characterization for 15 s during active welding and 3 filter samples were collected for mass concentration at T1, T3, and T5 for 5 min each.

The experiments were repeated in triplicate and samples were taken during each replicate to ensure reproducibility of the sample results. Averages and standard deviations were obtained for replicated measurements.

Results and Discussion

The welding simulations occurred in calm-air conditions. Air-movement measurements recorded were up to 0.05 m/s (~10 ft/min). These conditions are below the recommended acceptable comfort air motion at the worker of 0.25 m/s (~50 ft/min) (Ref. 15); however, welders often work in confined, poorly ventilated spaces where extremely low air movements are common. The temperature in the welding chamber was 23.8°C (74.8°F). The

inlets of the probes and the filters drew part of the aerosol-laden plume inside the sampling plenum. All conditions were held constant during the experiments with the exception of the horizontal distance from the welding arc and the sampling time. Horizontal measurements were taken at 30 and 200 cm from the welding arc. Assuming linear air movement, at the highest recorded air movements of 0.05 m/s, each measurement (from T1 to T6) represented potential exposure at an additional distance of 7.5 m from the source after each 150-s interval. Replicate measurements were taken at each sampling location to ensure reproducibility of the results. Background particle concentrations measured in the welding chamber with the CPC ranged between 2×10^3 and 2×10^4 particles/cc.

Figure 2 presents the variation in particle number distribution as a function of distance from the welding arc. These values represent averages over three replicates at 30 cm and three replicates at 200 cm from the arc at T1 during active welding. The error bars represent the standard deviation of the replicates and are indicative of the reliability of the generation system and of relatively small variations between replicates. Data between 400 and 600 nm was estimated by a straight-line segment to eliminate discontinuities in the curves; this data represents the interval of particle sizes not captured by the combined SMPS and APS instruments. Recorded number distributions at both distances present a similar shape with overlapping error bars and a main mode that peaks at about 200 nm. The principal distinction between the two measurements is in the presence of a secondary mode between 15 and 50 nm that only appeared at the shorter distance from the arc. This secondary mode is likely due to the high concentration of metal vapors near the arc, which quickly undergo condensation and coagulation upon being cooled to ambient temperatures (Ref. 2).

The mass distribution by particle size is presented in Fig. 3. Panel A of Fig. 3 represents the mass distribution at 30 cm from the source. The mass median aerodynamic diameter (MMAD) at this location is 350 nm (0.35 μm) and the geometric standard deviation is 1.5. Similar to the number distribution, at this shorter distance from the arc, the mass distribution is bimodal, with a secondary mode around 10 nm (0.01 μm). At this distance, there is also an increased amount of mass for particles larger than 1 μm that is attributable to the presence of spatter particles.

Panel B of Fig. 3 presents the mass distribution at 200 cm from the source. At this distance, the mass distribution is unimodal with MMAD of 299 nm (0.3 μm) and GSD of 1.367. Higher particle concentrations were expected at the distance closer to the arc (30 cm) compared to the greater distance (200 cm). Zimmer and Biswas (Ref. 2) observed that average particle number concentrations decrease with increasing distance from the arc between 5 and 20 cm. They measured 1.6×10^7 particles/cm^3 at 0–5 cm from the arc and 3.2×10^6 particles/cm^3 at 15–20 cm from the arc. In our experiments, we measured 2.7×10^6 particles/cm^3 at 30 cm from the arc and nearly identical concentrations (2.6×10^6 particles/cm^3) at 200 cm from the arc, indicating that at these distances while fresh welding fumes are being generated, the initial fast coagulation and condensation mechanisms observed by Zimmer and Biswas have slowed down and the particle distribution of the slow-moving plume is not changing substantially.

These findings have implications for second-hand exposure levels. While welding fumes are being actively generated, workers adjacent to the welding operator may be exposed to lower number concentrations of particles smaller than 100 nm; for particles larger than 100 nm, however, the measured exposures were similar at both locations. The samples collected near the welding arc also revealed the presence of spatter particles (larger than 1 μm) that contribute substantially to the mass measurements. These spatter particles were not found in the measurements taken at the greater distance.

Figure 4 presents the variation in particle number concentrations as a function of time. Panel A represents measurements taken at 30 cm from the welding source during active welding and at two subsequent intervals of 150 s. Panel B represents measurements taken at 200 cm from the source during active welding and at five subsequent intervals of 150 s. In both cases, once the welding process stopped, as the time interval increased, the average number concentrations gradually decreased and the size distribution shifted slightly toward larger particles. Each curve in Fig. 4 represents the average of three replicates of the same conditions and the error bars are the standard deviation of the three replicates. The width of the error bars indicate the conditions were highly reproducible in our experiments.

Each time interval in Fig. 4 corresponded with an increased residence time. As residence time increased, the concentration of particles decreased dramatically. This was especially marked for the small-diameter particles, as these particles coagulate onto larger particles and result in a shift in particle size distribution. A substantial decrease in nanoparticle concentrations can be observed after each time interval. For example, at 200 cm from the arc, the concentration of 95-nm particles during fume generation was about 1.1×10^6 particle/cm^3 and after 150 s it decreased to 6.5×10^5 particle/cm^3, or a 40% decrease. At the second time interval (300 s after welding), 95-nm particles decreased by an additional 38% and after 450 s these particles were further down to approximately 3.0×10^5 particle/cm^3, an additional 26% decrease. At the highest measured air velocity of 0.05 m/s, this 450-s residence time corresponds with a distance of approximately 20 m (65 ft) from the source.

Figure 5 shows electron microscopy images of the morphology samples collected. The left column in Fig. 5 (Panels A, B, and C) represents the morphology samples collected near the source. These samples contained large spheres (0.5–4 μm in diameter) generated by the welding spatter as well as smaller agglomerated particles. Particles collected 200 cm away from the source are presented on the right column of Fig. 5 (Panels D, E, and F). No spatter particles were found in the far samples and particle loading was substantially lower than that near the source. Primary-particle diameters were similar in both cases (10–200 nm in diameter); however, filter loadings appeared lower in the samples collected farther away from the source.

Average particle mass concentrations and standard deviations measured with the PTFE filters are reported in Table 1. The average mass concentration at 30 cm from the arc was 45 mg/m^3 (2.2 mg/m^3 standard deviation), five times higher than that measured at 200 cm from the source (9 mg/m^3 with 2.2 mg/m^3 standard deviation). The difference may be attributed to the presence of spatter particles near the source (Fig. 5, Panels B and C) that would contribute to most of the measured mass. These large spatter particles were not observed in

the morphology samples at the greater distance from the arc. At 200 cm from the arc, three mass measurements were taken at 5-min intervals. Mass concentrations at T3, 5 min after fume generation, decreased to 6.2 mg/m³ (2.3 mg/m³ standard deviation) and further to 5.4 mg/m³ (±1.3) at T5, 10 min after generation. These findings are consistent with those observed for particle size distributions (Fig. 4B), which show a decrease in particle concentrations over time.

Conclusions

In these experiments, we measured the spatial and temporal effects on fumes generated during gas metal arc welding. Particle size and mass distributions were measured and changes in particle morphology were investigated at two horizontal distances from the welding arc: 30 and 200 cm. The distance of 30 cm from the arc was selected as the typical distance of the breathing zone of a welder. The farther distance of 200 cm from the arc was selected as the distance of a potential nearby worker not directly involved in the welding process. The results of this investigation showed that during active welding, the overall particle number and mass distribution were very similar, with the difference that the welder may also be exposed to higher concentrations of particles smaller than 50 nm and to spatter particles (0.5–4 μm) generated during welding. Overall particle mass concentrations measured near the arc (30 cm) were five times greater than those measured at 200 cm from the arc. As time and distance increased after welding stopped and particles began settling, the particle concentrations decreased and the size distributions shifted slightly toward larger particles. Recommended exposure limits for welding fume and for the metals it may contain are expressed as mass concentrations and are not specific to number concentrations. Welding spatter particles appeared to be the principal component of mass concentrations; as a consequence, spatter may be a greater contributor to systemic dosage and thus to disease resulting from exposure to toxic metals. Our findings indicate that in terms of number concentrations, second-hand exposure to welding fumes at a distance of 200 cm (6.5 ft) from the welding arc may be as high as first-hand exposure. Therefore, it is also important to assess exposures to nearby workers and to pro tect those found to be exposed above applicable exposure limits.

These findings relate to experiments carried out in a controlled chamber with calm-air conditions, thus the exposure chamber results presented in this manuscript are most representative of confined, poorly ventilated spaces. Environmental and workplace factors such as air movement patterns will contribute to aerosol movements and may otherwise affect first- and second-hand exposures to welding fumes. Furthermore, these experiments highlight the importance of using local exhaust ventilation to capture welding fumes near their point of generation to not only reduce the welder's exposure but the exposure of nearby workers as well. Additionally, in light of these results, welders' helpers and other nearby workers in restricted work environments should wear the same level of respiratory protection as the welders. Future work should investigate exposures of welders and nearby workers under varying airflow rates.

References

1. Brand P, Lenz K, Reisgen U, Kraus T. Number size distribution of fine and ultrafine fume particles from various welding processes. Annals of Occupational Hygiene. 2013; 57(3):305–313. [PubMed: 23028013]

2. Zimmer AT, Biswas P. Characterization of the aerosols resulting from arc welding processes. Journal of Aerosol Science. 2001; 32(8):993–1008.

3. Cena LG, Chisholm WP, Keane MJ, Chen BT. A field study on the respiratory deposition of the nano-sized fraction of mild and stainless steel welding fume metals. Journal of Occupational and Environmental Hygiene. 2015; 12(10):721–728. [PubMed: 25985454]

4. Flynn MR, Susi P. Manganese, iron, and total particulate exposure to welders. Journal of Occupational and Environmental Hygiene. 2010; 7(2):115–126. [PubMed: 20013450]

5. Liu D, Wong H, Quinlan P, Blanc PD. Welding helmet airborne fume concentrations compared to personal breathing zone sampling. American Industrial Hygiene Association. 1995; 56(3):280–283.

6. Keane M, Stone S, Chen B. Welding fumes from stainless steel gas metal arc processes contain multiple manganese chemical species. Journal of Environmental Monitoring. 2010; 12:1133–1140. [PubMed: 21491680]

7. Keane M, Stone S, Chen B, Slaven J, Schwegler-Berry D, Antonini J. Hexavalent chromium content in stainless steel welding fumes is dependent on the welding process and shield gas type. Journal of Environmental Monitoring. 2009; 11(2):418–424. [PubMed: 19212602]

8. Cena LG, Chisholm WP, Keane MJ, Cumpstom A, Chen BT. Size distribution and estimated respiratory deposition of total chromium, hexavalent chromium, manganese and nickel in gas metal arc welding fume aerosols. Aerosol Science and Technology. 2014; 48(12):1254–1263. [PubMed: 26848207]

9. Antonini JM, Keane M, Chen BT, Stone S, Roberts JR, Schwagler-Berry D, Andrews R, Frazer DG, Sriram K. Alterations in welding process voltage affect the generation of ultrafine particles, fume composition, and pulmonary toxicity. Nanotoxicology. 2011; 5(4):700–710. [PubMed: 21281223]

10. Park RM, Bena JF, Stayner LT, Smith RJ, Gibb HJ, Lees PSJ. Hexavalent chromium and lung cancer in the chromate industry: A quantitative risk assessment. Risk Analysis. 2004; 24(5):1099–1108. [PubMed: 15563281]

11. Bowler RM, Nakagawa S, Drezgic M, Roels HA, Park RM, Diamond E, Mergler D, Bouchard M, Bowler RP, Koller W. Sequelae of fume exposure in confined space welding: A neurological and neuropsychological case series. NeuroToxicology. 2007; 28(2):298–311. [PubMed: 17169432]

12. Jankovic J. Searching for a relationship between manganese and welding and Parkinson's disease. Neurology. 2005; 64(12):2021–2028. [PubMed: 15985567]

13. Marconi M, Bravaccini A. Capture efficiency of integral fume extraction torches for GMA welding —Part 2. Welding in the World. 2010; 54(3–4):15–33.

14. Antonini JM, Afshari AA, Stone S, Chen B, Schwegler-Berry D, Fletcher WG, Goldsmith WT, Vandestouwe KH, McKinney W, Castranova V, Frazer DG. Design, construction, and characterization of a novel robotic welding fume generator and inhalation exposure system for laboratory animals. Journal of Occupational and Environmental Hygiene. 2006; 3(4):194–203. [PubMed: 16531292]

15. ACGIH. Industrial Ventilation: A Manual of Recommended Practice for Design. Cincinnati, Ohio: American Conference of Governmental Industrial Hyigienists Signature Publications; 2010.
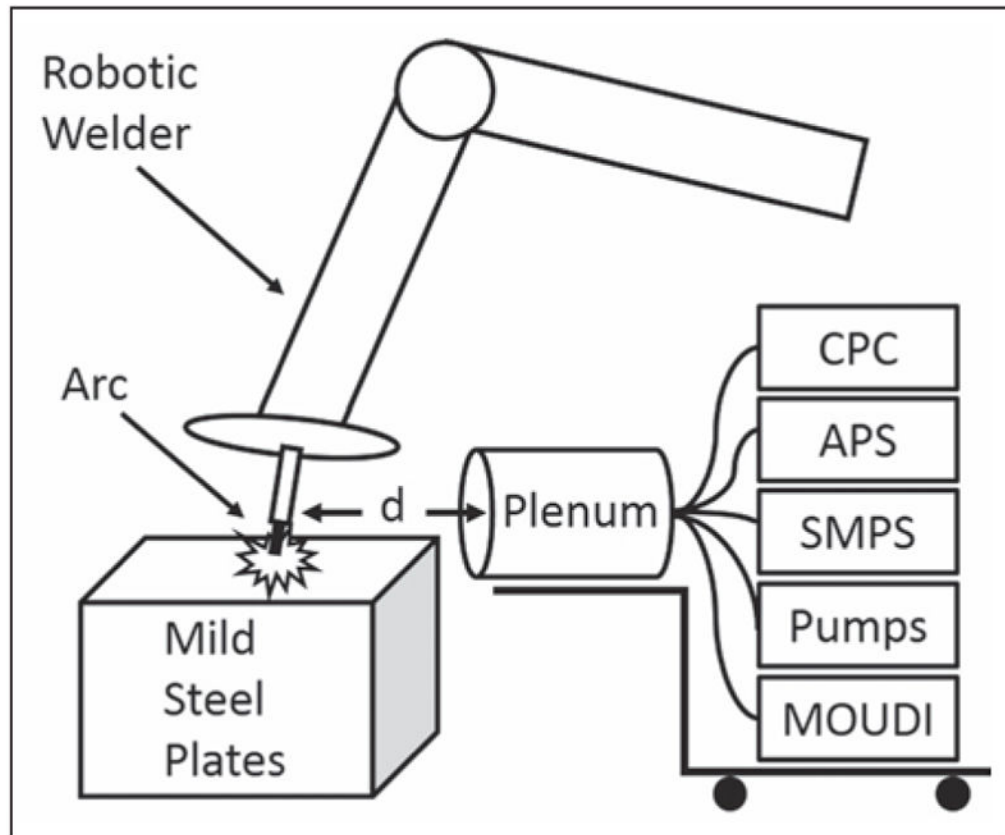
Fig. 1.
Experimental setup. CPC = condensation particle counter, APS = aerodynamic particle sizer, SMPS = scanning mobility particle sizer, MOUDI = micro-orifice uniform deposition impactor, and d = distance from the arc (30 or 200 cm).
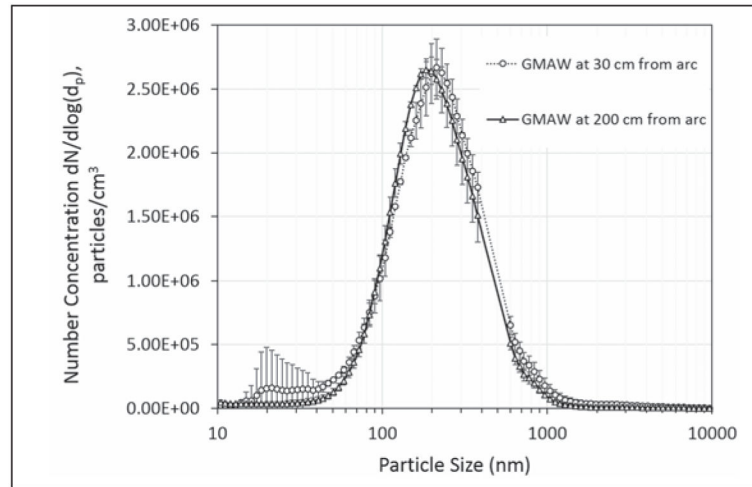
Fig. 2.
Number particle size distribution as a function of distance from the arc during active welding.
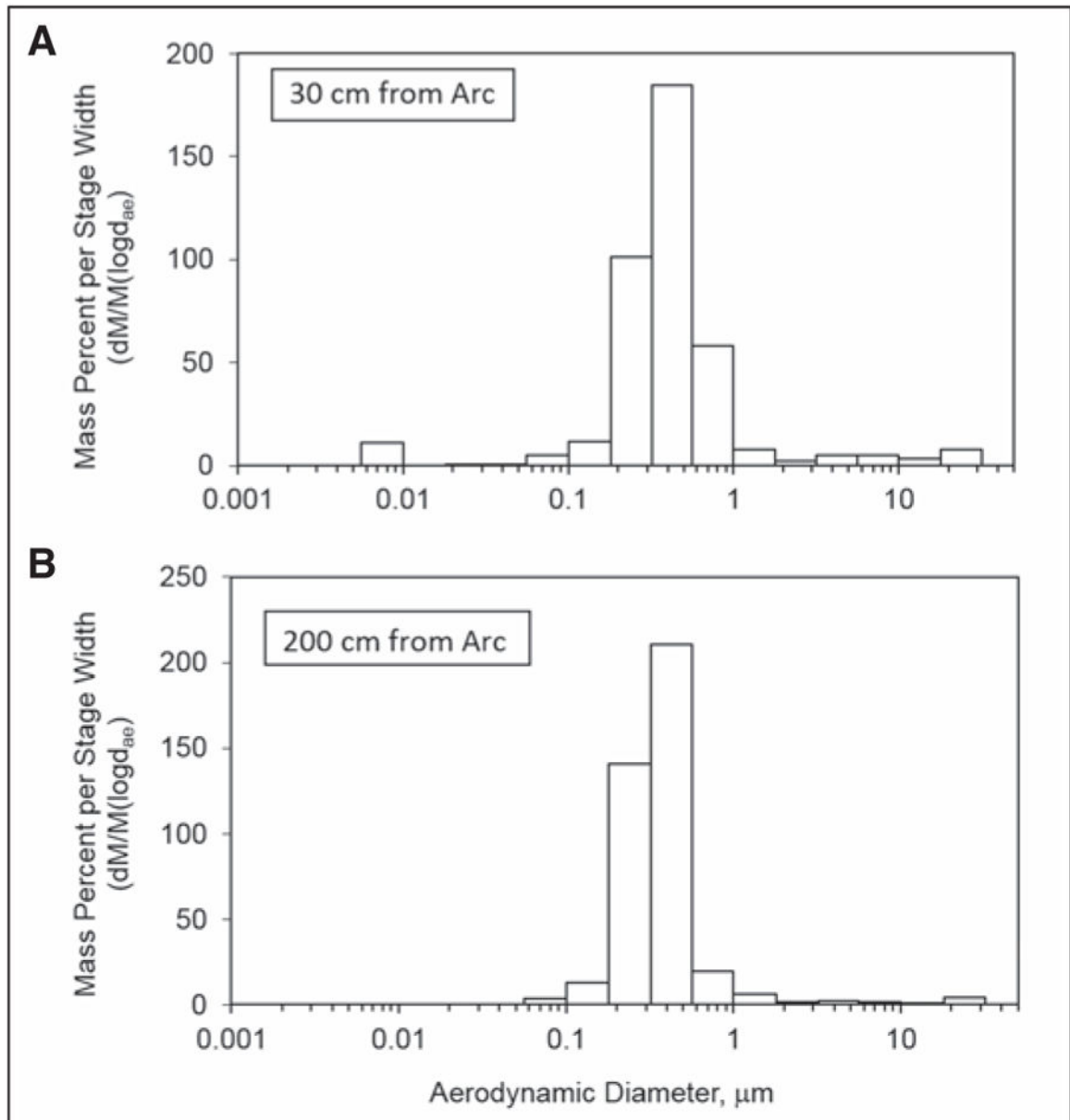
Fig. 3.
Mass distribution by size as measured with the MOUDI and nano-MOUDI impactor system at 30 cm from the arc (Panel A) and at 200 cm from the arc (Panel B).
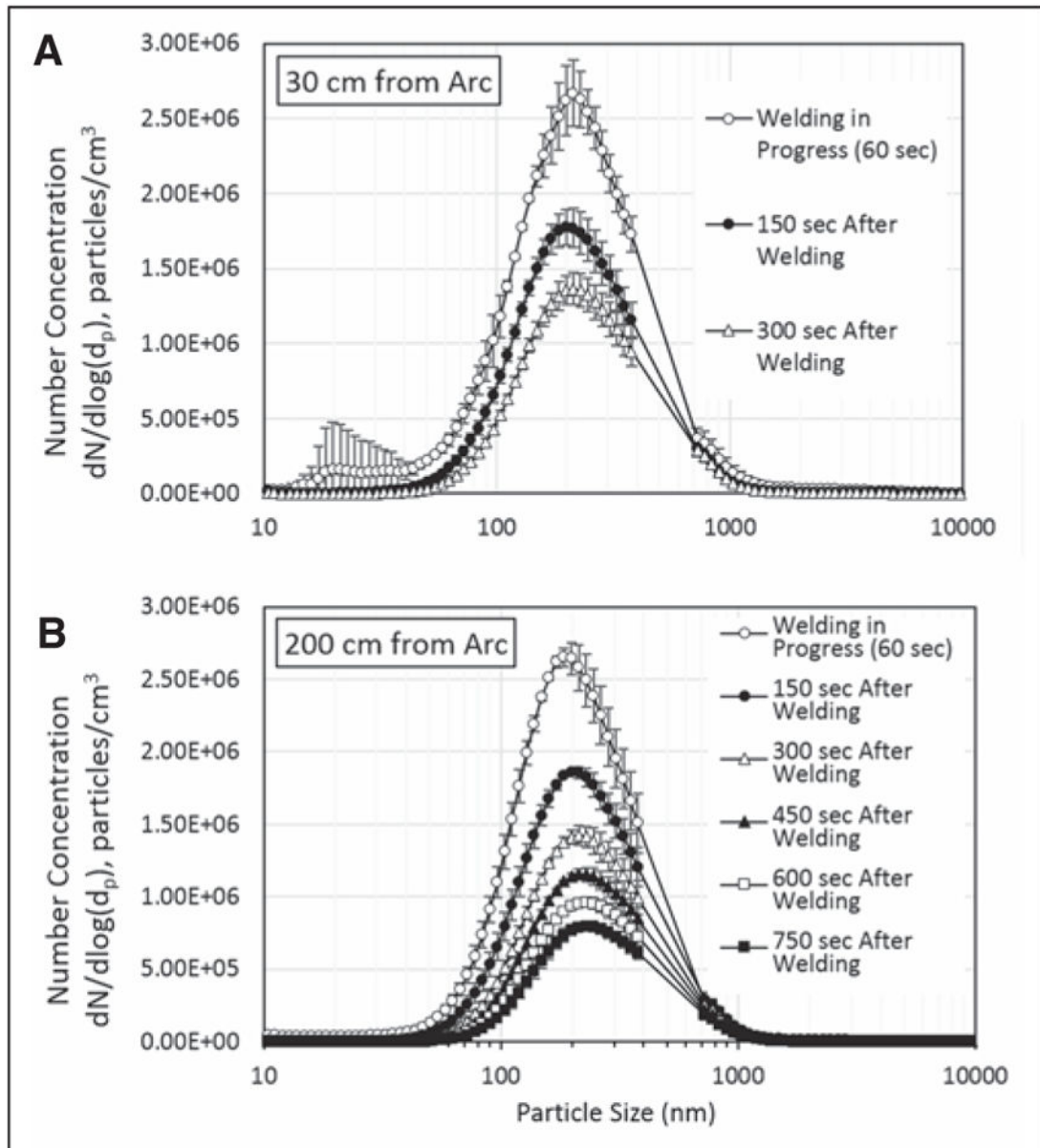
Fig. 4.
Number particle size distribution as a function of residence time as measured at 30 cm from the arc (Panel A) and at 200 cm from the arc (Panel B).
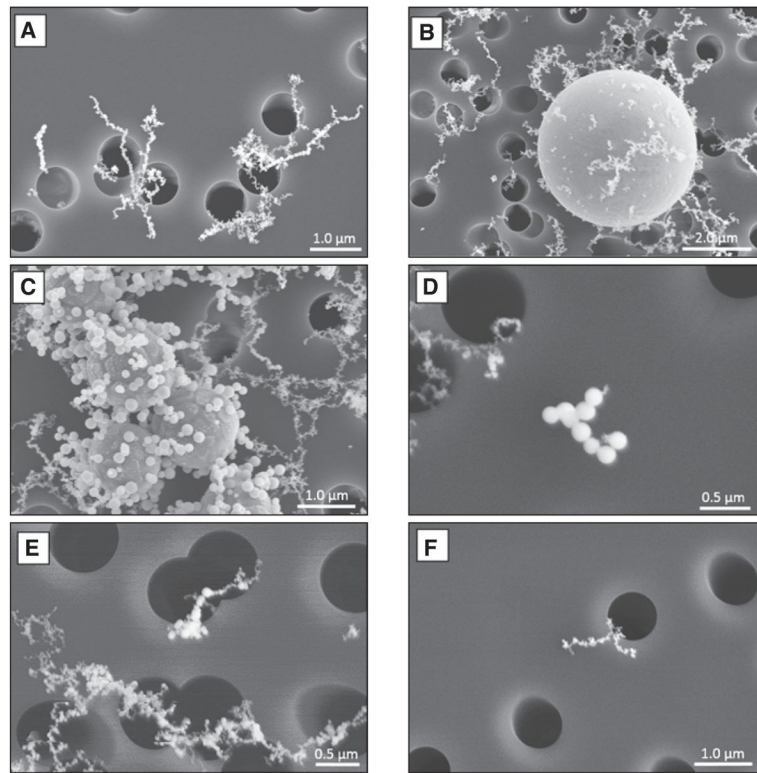
Fig. 5.
Scanning electron microscope images of the morphology samples collected at 30 cm from the arc (Panels A, B, and C) and at 200 cm from the arc (Panels D, E, and F).

Table 1

Averge Particle Mass Concentrations (mg/m^3) and Standard Deviation (SD) as a Function of Distance from the Arc and Time (Obtained from Gravimetric Analysis of Filter Samples)

Time	Near (30 cm)		Far (200 cm)	
	Mean	**SD**	**Mean**	**SD**
T1 (5 min)	45	2.2	9.0	2.2
T3 (T1 + 5 min)	n/a	n/a	6.2	2.3
T5 (T3 + 5 min)	n/a	n/a	5.4	1.3